JOURNAL OF Materials Feature Article CHEMISTRY

New directions in tin sulfide materials chemistry

Tong Jiang and Geoffrey A. Ozin*

Materials Chemistry Research Group, Lash Miller Chemical Laboratories, University of Toronto, Toronto, Ontario, Canada, M5S 3H6

Tin sulfide-based materials can exist in many forms, ranging from discrete molecular species, to 1D chains, 2D dense and porous sheets and 3D open frameworks. The local coordination geometry around a tin center may vary from trigonal pyramidal, to tetrahedral, trigonal bipyramidal and octahedral, and around sulfur from terminal, v-shaped to trigonal pyramidal. The oxidation state may take +2 and +4 for tin and −2, −1, 0 for sulfur. The tin sulfide chemistry is further enriched by the catenation ability of sulfur. In addition, other elements (metal and non-metal) can be incorporated into the tin sulfide structures to yield ternary and quaternary materials. More importantly, using the recent developed 'soft chemistry' synthetic approach, various novel porous tin (poly)sulfide materials have emerged that display interesting optical, electrical and adsorption properties. Representative tin sulfide materials will be presented and discussed in this review to demonstrate the development of tin sulfide chemistry in the last three decades.

1.0 Introduction

Attributed to the versatile coordinating characteristic of tin and sulfur, tin sulfide-based solid state materials exhibit a rich structural chemistry.[1] As a main group 14 element on the fifth row of the Periodic Table, a tin atom can take a coordination number of 2 to 9, and as a result, the environment around tin embraces many geometrical arrangements. The most common ones are trigonal pyramidal for divalent tin, and tetrahedral, trigonal bipyramidal and octahedral for tetravalent tin.[2] Sulfur, a main group 16 element on the third row of the Periodic Table, displays an equally diverse coordination chemistry as tin. In addition sulfur chemistry is adorned by the catenation ability of sulfur. The catenation length can be as short as in S_2 and as long as in a polymeric sulfur chain which may contain more than 200 000 sulfur atoms.[3] One may think of numerous ways to link tin and sulfur and/or polysulfur together with different coordination geometries around the tin and sulfur sites. In the past three decades, various synthetic approaches, including solid state reactions,[4] hydrothermal or organothermal[5] synthesis, and molten salt (flux) methods,[6] have been employed and developed in the search for new tin sulfide and/or polysulfide-based solid state materials, especially those with open-framework structures. As a result, many new discrete molecular and 1D chain, 2D sheet and 3D frameworks have emerged and some of them present interesting optical and electrical properties for device applications.[7] It has proven possible to incorporate other elements into the tin sulfide- and polysulfide-based structures, to form ternary or quaternary structures. As tin has stable positive oxidation states of two and four, mixed-valence tin(II,IV) structures are also known. In what follows, a brief summary of each structure type will be presented to exemplify the achievements of tin sulfide and polysulfide materials chemistry over the last thirty years, and to demonstrate the structural diversity of these materials. The large family of organotin sulfide compounds, although important and fascinating in their own right, tend to be molecular, low melting, volatile and soluble in organic solvents and on this basis they are considered distinct from the solid state tin sulfides and are therefore excluded from this survey.

2.0 Tin sulfide molecules and chains

In discrete molecular tin(IV) thiostannate anions, tin centers often display a tetrahedral geometry as shown in Fig. 1 for monomeric[8] $(SnS_4)^{4-}$, dimeric[9,10] $(Sn_2S_6)^{4-}$ and $(Sn_2S_7)^{6-}$ species. In $(SnS_4)^{4-}$, regular T_d symmetry exists around the tin(IV) site, while in $(Sn_2S_6)^{4-}$ and $(Sn_2S_7)^{6-}$, a distorted tetrahedral geometry is present. The versatile bonding characteristic of tin sulfide-based structures is evident in the two dimeric tin(IV) thiostannate anions $(Sn_2S_6)^{4-}$ and $(Sn_2S_7)^{6-}$. Both anions are constructed from two SnS_4 tetrahedra, through corner-sharing in $(Sn_2S_7)^{6-}$ and edge-sharing in $(Sn_2S_6)^{4-}$. The preparation and structure of tetrameric $(Sn_4S_{10})^{4-}$ have been reported by Krebs.[1b] The tetrameric anion consists of four corner-sharing SnS_4 tetrahedral units with an adamantane geometry cluster. The stability of these tin(IV) thiostannates in aqueous solution is believed to be pH dependent and generally a lower pH favors higher oligomers or polymers.[1b] For example, both Na_4SnS_4 and $Na_4Sn_2S_6$ can be prepared by dissolving freshly precipitated SnS_2 in an aqueous solution of Na_2S; however, the pH for the crystallization of Na_4SnS_4 is around 11, while that for $Na_4Sn_2S_6$ is around 9.

One can imagine that if a terminal sulfur on each tin site in the dimeric $(Sn_2S_7)^{6-}$ anion coordinates to another $(Sn_2S_7)^{6-}$ and this process continues indefinitely, a polymeric tin(IV) thiostannate chain would be created. Indeed, this type of tin(IV) thiostannate, $(SnS_3)^{2-}$ polymer chain has been crystallized from a reaction mixture of KOH, H_2S and SnS_2 in aqueous solution, the single crystal structure of which is shown in Fig. 2.[11] In $(SnS_3)^{2-}$ a monomeric SnS_4 building unit shares two corners with two neighbouring units. The charge-balancing K^+ cations and occluded water molecules reside between the polymeric $(SnS_3)^{2-}$ chains. An extended hydrogen-bonding network is produced through the involvement of terminal sulfur and occluded water.

Tin sesquisulfide, Sn_2S_3, is one of the tin sulfide minerals, and named ottemannite after its discovery by the German mineralogist J. Ottemann.[12] In the laboratory, acicular crystals of this material can be prepared by heating a stoichiometric mixture of elemental Sn and S powders at 720 °C in a sealed quartz tube.[13] Sn_2S_3 is the best known mixed-valence tin sulfide compound and has an aesthetic ribbon structure as shown in Fig. 3. The tin(IV) sites in the ribbon are octahedrally coordinated with Sn—S distances of 2.459–2.604 Å. The tin(II) sites on the edge of the ribbon have a typical trigonal pyramidal geometry with two Sn—S distances of 2.645 and 2.765 Å. At least three 'polytypes' of Sn_2S_3, *i.e.* α-$Sn_{2\pm x}S_3$, β-$Sn_{2\pm x}S_3$ and γ-Sn_2S_3, have been identified. Moh has examined the phase diagram of tin sulfide systems and related minerals, and

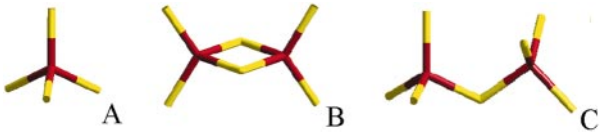

Fig. 2 An illustration of the zig-zag chain structure of $K_2SnS_3 \cdot 2H_2O$11 with the K^+ and water molecules omitted for clarity

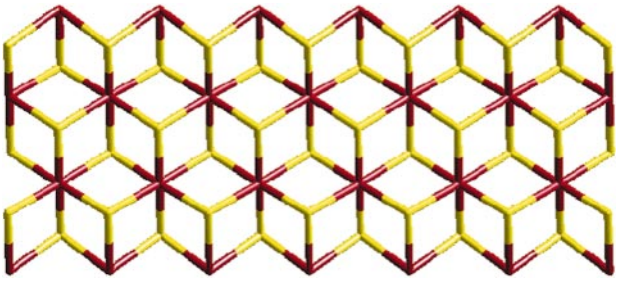

Fig. 3 A representation of the ribbon structure of Sn_2S_3,13 the trigonal-pyramidal tin(ii) locating at the edge and the octahedral tin(iv) at the center of the ribbon

reported that the non-stoichiometric α-$Sn_{2\pm x}S_3$ and β-$Sn_{2\pm x}S_3$ phases exist above 700 °C, while the γ-Sn_2S_3 phase is stable below 675 °C.12 However, there are incidents for which the Sn_2S_3 phases do not fall into the right region of Moh's phase diagram.13 Isostructural PbIISnIVS$_3$ and SnIIGeIVS$_3$ have al been synthesized under similar conditions.

3.0 Tin sulfide layers

In general, tin sulfides favor a two-dimensional structure. Quite a few layered structure types have been reported, with various combinations of tin and sulfur local coordination geometries. The topology of tin sulfide sheets may feature a close-packing or an open structure which is decorated by regular arrays of pores with a variety of geometric shapes and sizes circumscribed by the tin and sulfur components. The sheet itself may be flat or undulated. A summary of representative 2D tin sulfide structures is given in Table 1.

3.1 Tin monosulfide

Tin monosulfide, also called herzenbergite, was first reported by the German mineralogist R. Herzenberg.[14] Single crystals of this material can be prepared by reacting stoichiometric Sn and S elements over a temperature range of 600–750 °C.[14] At room temperature, tin monosulfide adopts the GeS structure. The corrugated tin sulfide double layers are displayed in Fig. 4. Each tin atom is coordinated by six sulfurs in a highly distorted

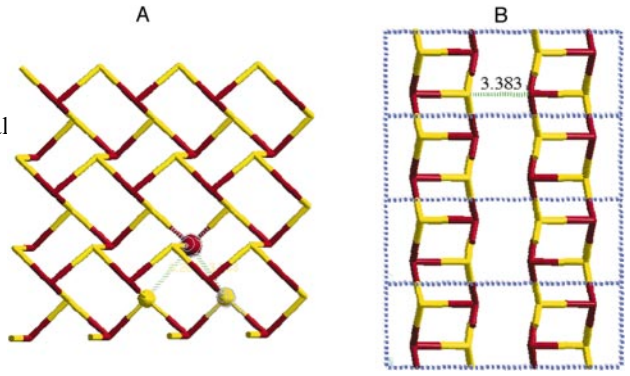

Fig. 4 A representation of the layered structure of SnS with one distorted SnS_6 octahedron highlighted (note that the sixth sulfur apex on the neighboring tin sulfide layer is not shown)[15]

octahedral geometry. As the octahedra are so distorted the tin atom is actually displaced toward one of the faces of the octahedra as shown in Fig. 4. This leads to three short Sn—S bonds of *ca.* 2.7 Å and three long Sn—S bonds of almost 3.4 Å. There are two SnS layers in one unit cell and one of the long distance sulfurs actually resides on the neighboring SnS layer. This weak Sn—S interaction binds the two tin sulfide layers together to form a double-layer structure. Tin monosulfide undergoes a complicated thermal expansion from room tem-

Table 1 A summary of representative 2D tin sulfide structure types

chemical formula	coordination number		character of tin sulfide layer	synthetic technique
	Sn	S		
SnS	6	3	dense, undulated	high temperature
SnS_2	6	3	dense, flat	CVT
$Rb_2Sn_3S_7 \cdot 2H_2O$	4, 6	2, 3	porous, flat	hydrothermal
$Cs_4Sn_5S_{12} \cdot 2H_2O$	5, 6	2, 3	porous, flat	hydrothermal
SnS-1 ($Cat_2Sn_3S_7$)	5	2, 3	porous, flat	hydrothermal
SnS-3 ($Cat_2Sn_4S_9$)	4, 5	2, 3	porous, undulated	hydrothermal

perature to *ca.* 605 °C at which temperature it transforms to the TlI structure type. This solid state phase transition is accompanied by a continuous movement of Sn and S along the entire [1 0 0] direction in the unit cell. An intralayer optical A_g phonon softening mechanism has been proposed to explain this polymorphic phase transition. Non-stoichiometric $Sn_{1\pm x}S$ phases have also been reported with a wide variety of unit cell dimensions.[12]

3.2 Tin disulfide and polytypism

Tin disulfide is probably the first known tin sulfide material, the laboratory synthesis of which can be traced back some two hundred years.[15] Crystals of SnS_2 are typically prepared through the chemical vapor transport technique (CVT) over a temperature range of 600–800 °C, with I_2 as a transport agent.[16] Tin disulfide adopts the PbI_2 layered structure with a hexagonal unit cell, in which tin atoms are located in the octahedral sites between two hexagonally close-packed sulfur slabs to form a sandwich structure, as shown in Fig. 5. The SnS_2 layer can be viewed as composed of all-edge-sharing octahedral SnS_6 building units with the sulfurs exhibiting three-coordination and local trigonal-pyramidal symmetry. The SnS_2 layers are then stacked on top of one other along the crystallographic *c*-axis and held together by weak van der Waals forces. There are many ways to stack these layers together to create various polytypes. More than 70 polytype structures of SnS_2 have been established through a complicated single crystal structure analysis procedure. All of the polytypes have the same hexagonal close-packed structure within the layer, and therefore an identical unit cell parameter *a* of 3.647 Å; however, they exhibit a different parameter *c* orthogonal to the layer which is an integral number of the interlamellar spacing 5.899 Å.[17] Some polytypes may have a giant unit cell with a very large *c* parameter, as they contain many tin sulfide layers in one unit cell. For example, the polytype 258 R_1 contains as many as 258 tin sulfide sheets in one unit cell, with a *c* parameter of 761 Å![18] It should be mentioned that one crystallite of SnS_2 often contains domains of different polytypes, and the structural details of one polytype have to be extracted from a crystal of mixed phases. Therefore, the determination of an SnS_2 polytype structure has never been a trivial task.[19,20]

Recently, Palosz proposed that the polytypes of SnS_2 originate from the partial occupancy of the tin and sulfur sites in the SnS_2 crystal.[21] Through measuring the density of SnS_2 polytype crystals, he found that the overall occupancy of tin and sulfur in some polytypes can be as low as 80%. He attributed the different stacking sequences of tin sulfide layers to the occupancy deficiency level of the tin sulfide layers. In view of the many stoichiometries of tin and sulfur in stable tin sulfide materials, like SnS, Sn_2S_3, Sn_4S_5 and SnS_2, Polasz suggested that it is the versatile bonding nature of tin and sulfur that is responsible for the many stoichiometric, non-stoichiometric and lattice site-deficient structures of tin sulfides, and the occurrence of polytypes.

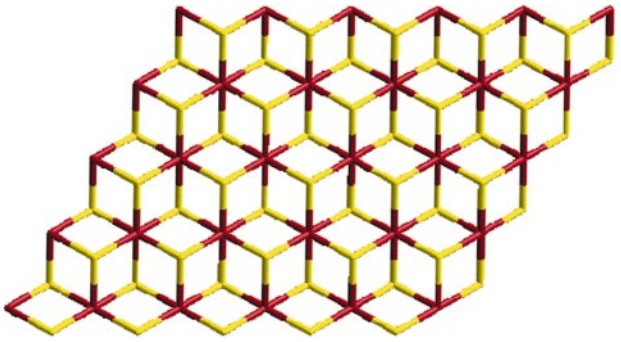

Fig. 5 A representation of the dense-packed layered structure of SnS_2 [16]

3.3 $Rb_2Sn_3S_7\cdot 2H_2O$

Single crystals of $Rb_2Sn_3S_7\cdot 2H_2O$ have been prepared by hydrothermal treatment of SnS_2 and Rb_2CO_3 in a H_2S saturated aqueous solution at 190 °C.[22] As displayed in Fig. 6, it contains layered thiostannate $(Sn_3S_7)^{2-}$ anions with octahedral SnS_6 and tetrahedral SnS_4 units. The $(Sn_3S_7)^{2-}$ anions are partially constituted by chains of the SnS_6-based dense structure as found in bulk tin(IV) disulfide, (Fig. 5), plus Sn_2S_6-based open structures. One way to view these $(Sn_3S_7)^{2-}$ sheets is that the original close-packed SnS_2 layer is dissected after every two rows of octahedral SnS_6 units and then sewed together by Sn_2S_6 chains, Fig. 6, to create an open 2D structure. The tetrahedral tin and double bridge $(\mu\text{-S})_2$ sulfur linkages (in green), *i.e.* the $Sn(\mu\text{-S})_2Sn$ units of the Sn_2S_6 chains are found to be disordered with an overall occupancy of 0.5 in the single crystal structure. The disorder of the Sn_2S_6 chains illustrates the versatile bonding character of tin sulfide-based structures. One can imagine that the three-coordinated sulfur from the Sn_2S_6 chains in Fig. 6 are sometimes two-coordinated, due to the 0.5 partial occupancy of the $Sn(\mu\text{-S})_2Sn$ unit. However, these different coordination environments are happily sharing one unit cell position. The 8-atom-membered rings shown in Fig. 6 can also randomly assume many different sizes. The rigid structure of SnS_2 is now attached to flexible and open Sn_2S_6 structure units. The physical properties, especially small molecule adsorption character, of this material, should be very interesting.

3.4 $Cs_4Sn_5S_{12}\cdot 2H_2O$

When Rb_2CO_3 was substituted by Cs_2CO_3 in the above reaction mixture for $Rb_2Sn_3S_7\cdot 2H_2O$, a new tin(IV) sulfide material, $Cs_4Sn_5S_{12}\cdot 2H_2O$, was crystallized at 130 °C.[23] It has a 2D porous layer structure, consisting of octahedral and trigonal bipyramidal tin sites, Fig. 7. The basic building unit in bulk SnS_2 can also be found in this structure. In SnS_2, three all-edge-sharing octahedral SnS_6 units create a Sn_3S_4 broken-cube building block. Therefore, the layered structure of SnS_2 can be envisioned as being built from these edge-sharing Sn_3S_4 broken cubes. In $(Sn_5S_{12})^{4-}$, two of the primary Sn_3S_4 broken cubes are linked together by sharing one octahedral tin to yield double Sn_3S_4 secondary broken-cube building blocks. They are further connected through double bridge $Sn(\mu\text{-S})_2Sn$ sulfur bonds to create the 20-atom-membered rings found in the 2D porous layers of $(Sn_5S_{12})^{4-}$. It is interesting to note that a larger pore has been created when the size of the charge-balancing cation is increased from Rb^+ to Cs^+. The other point worth mentioning is that by reducing the reaction temperature below 200 °C, the open-layered structures of

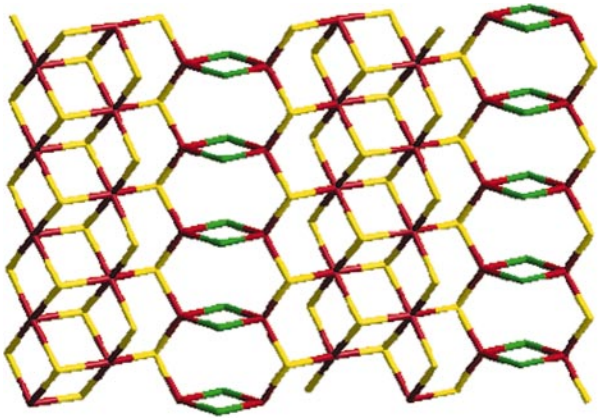

Fig. 6 A representation of the 2D structure of $Rb_2Sn_3S_7\cdot 2H_2O$, the Rb^+ and water molecules are omitted for clarity. The tetrahedral tin and attached double bridge $Sn(\mu\text{-S})_2Sn$ sulfurs (in green) are disordered with a partial occupancy of 0.5.[22]

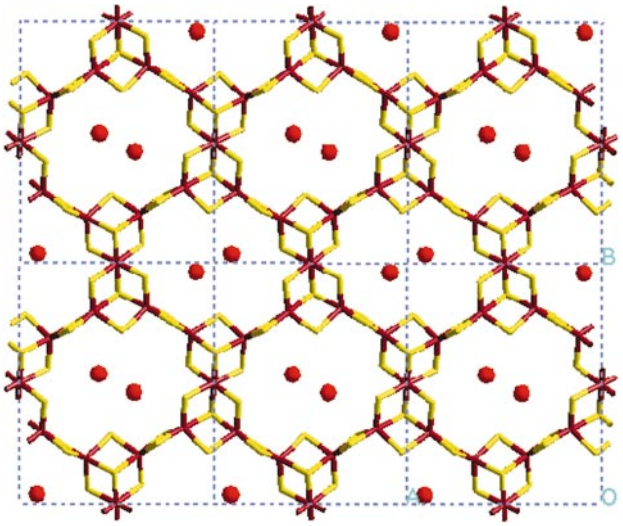

Fig. 7 A representation of the 2D open structure of $Cs_4Sn_5S_{12}\cdot 2H_2O$, the caesium cations and water are omitted for clarity. The 20-membered elliptical rings are parallel to the (0 0 1) plane.[23]

$Rb_2Sn_3S_7\cdot 2H_2O$ and $Cs_4Sn_5S_{12}\cdot 2H_2O$ are created, in contrast to the dense layered structure of SnS_2, which is crystallized at temperatures above 600 °C. This exemplifies the 'soft chemistry approach' to new, open framework solid state materials.

3.5 SnS-1 and SnS-3

The above two open-framework tin(IV) thiostannate materials are built entirely of inorganic components with alkali metal cations, Rb^+ and Cs^+, as counter ions. It has proven feasible to employ organic cations as charge balancing moieties for the assembly of new open-framework structures.[5a] For example, 2D porous materials, R-SnS-1 $[(Cat^+)_2Sn_3S_7]$ and R-SnS-3 $[(Cat^+)_2Sn_4S_9]$, have been prepared in the presence of a large variety of tetraalkylammonium and amine molecules under hydrothermal reaction conditions, where R represents the occluded organic cations. The basic building blocks of these two materials are the same Sn_3S_4 broken cube as found in $Cs_4Sn_5S_{12}\cdot 2H_2O$, but, with different connectivity. In SnS-1, the Sn_3S_4 broken cubes are joined together by double bridge Sn(μ-S)$_2$Sn sulfur bonds to form hexagonally shaped 24-atom rings, Fig. 8, and in SnS-3 by double bridge Sn(μ-S)$_2$Sn sulfur bonds as well as tetrahedral SnS_4 spacer units to form elliptically shaped 32-atom rings, Fig. 9. The tin atoms in SnS-1 materials feature a single kind of distorted trigonal-bipyramidal site,

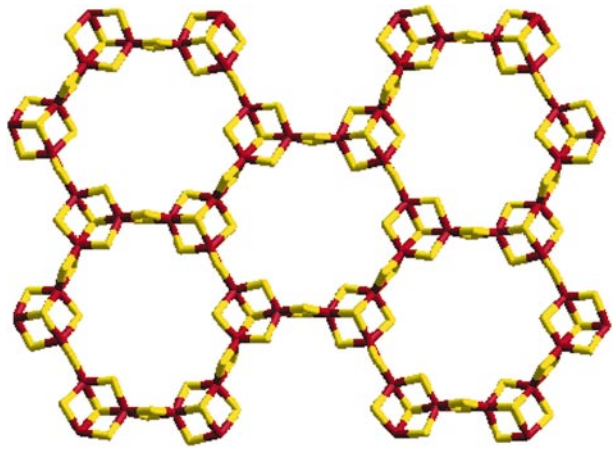

Fig. 8 A representation of the 2D open structure of $(Me_4N)_2Sn_3S_7\cdot H_2O$, the Me_4N^+ cations and H_2O molecules are omitted for clarity. The 24-membered hexagonal rings are parallel to the (1 0 1) plane.[26]

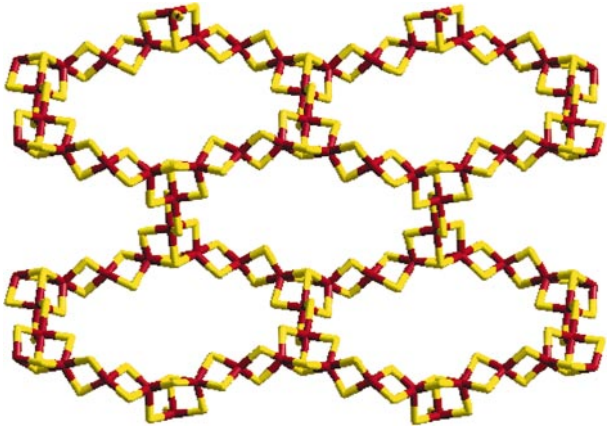

Fig. 9 A representation of the 2D open structure of $(Pr^n_4N)_2Sn_4S_9$, the $Pr^n_4N^+$ cations are omitted for clarity. The 32-membered elliptical rings are parallel to the (1 0 1) plane.[28]

while those in SnS-3 display both distorted trigonal-bipyramidal and tetrahedral symmetries. The diversity of tin sulfide bonding patterns is evident in these materials. Note that the tin thiostannate layer, $(Sn_3S_7)^{2-}$, in SnS-1 has an identical composition to that of $Rb_2Sn_3S_7\cdot 2H_2O$, Fig. 6, although the macroscopic structures of these two materials are completely different.

Various SnS-1 and SnS-3 materials, with different space groups, layer spacings and stacking sequences, have been obtained in the presence of a range of template cations. For example, *tert*-butylammonium,[24] Me_3HN^+,[25] Me_4N^+,[26] NH_4^+/Et_4N^+,[27] Et_4N^+,[27] $DABCOH^+$[27] and quinuclidinium[24] have all resulted in the SnS-1 structure; while $Pr^n_4N^+$ and $Bu^n_4N^+$ resulted in SnS-3.[28] A comparison of some of the SnS-*n* materials is given in Tables 2 and 3. It is evident that in the assembly of the SnS-*n* materials, the organic cations appear to have a particular kind of templating function. The 24-atom rings present in the SnS-1 structure are templated by smaller cations, while the 32-atom rings present in the SnS-3 structure by larger cations. The interlamellar spacing is about 8.5–9 Å in the SnS-1 structure, and about 14 Å in the SnS-3 structure. The pore size and interlamellar spacing among the various SnS-*n* families of materials also display certain correspondence with the size of the template cations as summarized in Tables 2 and 3. Interestingly, as described above, the Cs^+ cation with a radius of 1.81 Å has templated the open layered structure of $Cs_4Sn_5S_{12}$, in which 20-atom rings are present in the tin(IV) sulfide layer with an interlamellar spacing of 7.166 Å. However, in the presence of cyclooctasulfur molecules, Cs-SnS-1 ($Cs_2Sn_3S_7\cdot 1/2S_8$) has been synthesized.[29] Cs-SnS-1 is isostructural with $(DABCOH)_2Sn_3S_7\cdot H_2O$. The Cs^+ cations are located between the tin sulfide gaps to give an interlamellar distance of 8.151 Å. The 24-atom rings are occupied by cyclooctasulfur rings which cannot be removed without harming the integrity of the tin sulfide framework. It appears that the cyclooctasulfur molecule functions as a co-templating agent with the Cs^+ cation, and the Cs^+ alone is not large enough to direct the formation of the SnS-1 structure. The cations in the open-framework tin chalcogenides appear to have a charge-balancing, space-filling and structure-directing role, possibly analogous to the templating properties of cations in the synthesis of zeolites and molecular sieves.

It is interesting to mention that the remarkable structural differences among the R-SnS-1 and R-SnS-3 families of materials indicate that the bonding between tin and sulfur, and thus the constituent $[Sn_3S_7]^{2-}$ and $[Sn_4S_9]^{2-}$ tin(IV) sulfide layers, is extremely flexible. As summarized in Tables 2 and 3, the shape and size of the 24-atom rings in the SnS-1 and the 32-atom rings in the SnS-3 structures, as well as the layer stacking sequence and interlamellar spacings, can be modified

Table 2 A summary of the dimensions of the 24-atom rings and the interlayer spacing and layer stacking sequences of various SnS-1 materials

R-SnS-1 material	space group	pore dimensions[a] /Å × Å × Å	interlamellar spacing/Å	stacking sequence
$Cs_2Sn_3S_7{\cdot}0.5S_8$	$C2/c$	$10.79 \times 10.79 \times 10.47$	8.151	AB
$(Me_4N)_2Sn_3S_7{\cdot}H_2O$	$P2_1/n$	$11.69 \times 11.03 \times 9.69$	8.511	AA
$(DABCOH)_2Sn_3S_7{\cdot}H_2O$	$C2/c$	$10.98 \times 10.98 \times 9.95$	8.594	AB
$(NH_4)_{0.5}(Et_4N)_{1.5}Sn_3S_7$	$P3_121$	$10.94 \times 10.94 \times 10.88$	9.011	ABC
$(Et_4N)_2Sn_3S_7$	$P2_1/n$	$11.58 \times 10.84 \times 10.42$	8.915	AA

[a]Dimensions are defined from sulfur center to sulfur center as illustrated in Fig. 8.

Table 3 A comparison of TPA-SnS-3 and TBA-SnS-3 structures

	TPA-SnS-3	TBA-SnS-3
formula	$(Pr^n{}_4N)_2Sn_4S_9$	$(Bu^n{}_4N)_2Sn_4S_9$
space group	$P2_1/n$	$Pbcn$
pore dimensions[a]/Å	20.65×9.32	19.8×11.3
interlamellar dimension/Å	14.05	14.2
layer stacking sequence	AA	AB

[a]Dimensions defined as sulfur center to sulfur center as illustrated in Fig. 9.

considerably in response to the change of size and shape of the organic templates. This phenomenon may explain the relatively smaller structural variety so far observed for microporous tin(IV) sulfide-based materials in comparison with the myriad of structure types for the microporous oxide-based relatives like zeolites and aluminophosphates. In order to accommodate the size/shape changes of templates, the microporous layers of the tin(IV) sulfide materials undergo elastic deformation to alter the void spaces within and between the layers, rather than forming a completely new microporous structure type. This is to be contrasted with 3D microporous structures, in which there exists a greater restriction on the size and shape of the void space, either a cavity or channel, which can barely be deformed without an accompanying complete reorganization of the 3D framework. However, it should be mentioned that the 3D open frameworks of RHO and ZSM-5 zeolite materials have been found to display interesting framework flexibility similar to that described for the 2D SnS-*n* materials.[30] It has also been shown that a similar structural flexibility of the R-SnS-*n* structures can be induced by pressure[27] and adsorbed guest molecules with a concomitant, drastic electrical property change.[27,31] In addition, attributed to the 2D open structure nature of the SnS-*n* materials, they are found to display unique adsorption behaviour towards guest molecules. For example, they may behave like a microporous material and/or an intercalation host. In other words, the adsorption of guest molecules in the SnS-*n* materials is controlled by both the size/shape and the properties of guest molecules. The unique structural flexibilty and adsorption properties of these materials make them of considerable interest as potential chemoselective sensory element for molecular recognition devices.[7,31]

It is interesting to note that the framework flexibility of the SnS-*n* materials is related to the well known polytype phenomenon occurring in bulk SnS_2. They all originate from the flexible bonding nature of tin(IV) and sulfur(−II) centers. However, the constituent tin sulfide layers in different SnS_2 polytypes are identical and all of the polytypes have the same 2D unit cell parameters and structure within the tin sulfide sheet. The only difference among them is the stacking sequence of the constituent layers and the cell parameter along the stacking direction. In this regard, different SnS-1 or SnS-3 structures have different 3D cell parameters and space groups. Furthermore, the tin sulfide constituent layer in each particular structure has unique Sn−S bond angles and distances, and therefore a distinct pore size and shape. It appears that the regular microscopic perforations of the tin sulfide layer have brought additional flexibility to the tin sulfide-based layered structures.

3.6 Tin sulfide–organic composite mesophases

Thermotropic tin(IV) sulfide–organic composite semiconductor materials have been synthesized recently in the presence of long-chain amine molecules.[27,32a] The as-synthesized crystalline form of Meso-SnS-1 is established to have a structure that is based upon well registered yet poorly ordered porous tin(IV) sulfide layers with a layer spacing of 50 Å, between which are sandwiched well organized hexadecylamine bilayers, Fig. 10. This material displays interesting thermal transitions upon heating. On warming this material to around 45 °C the hexadecylamine bilayer first becomes disordered while the porous tin(IV) sulfide sheets remain registered. This is followed, around 85 °C, by a transition where both the alkylamine bilayer and the porous tin(IV) sulfide lamellae become liquid crystalline at which point the intralayer but not the interlayer registry is lost. The liquid crystal organic–inorganic composite phase has either a nematic or a smectic C structure. Electrically, the room temperature ordered phase of Meso-SnS-1 has a conductivity of $5.3 \times 10^{-8}\ \Omega^{-1}\,cm^{-1}$ which increases by more than 1000 times on transforming to the LC phase where it behaves as a semiconducting metallogen. The conductivity of Meso-SnS-1 cycles reversibly with temperature and displays discontinuities that are coincident with the crystal–semiliquid crystal and semiliquid crystal–liquid crystal thermal transitions. Meso-SnS-1 can readily form electrically conducting thin films which are able to reversibly adsorb molecules like H_2O and CO_2. These properties bode well for the use of this new class of

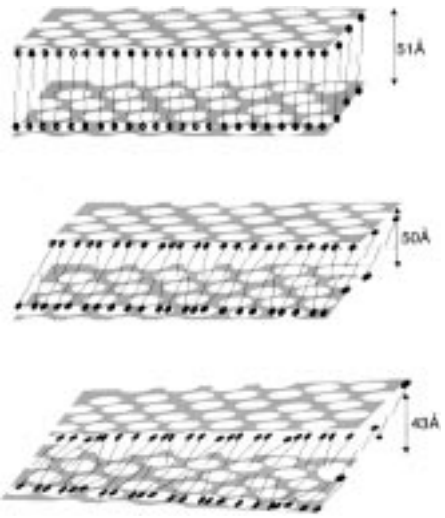

Fig. 10 Illustration of the structures of the as-synthesized crystalline porous layer form of mesomorphic tin(IV) sulfide (top) and its semi-liquid and liquid crystalline phases. On warming the material the alkylamine bilayer first becomes disordered around 45 °C while the porous tin(IV) sulfide sheets remain more-or-less registered (middle), and then around 85 °C, both the alkylamine bilayer and the porous tin(IV) sulfide lamellae become liquid crystalline at which point the intralayer but not the interlayer registry is lost (bottom).[32]

inorganic–organic semiconducting LCs for electro-optical displays and chemical sensing applications. The advantages of thermotropic Meso-SnS-1 over the R-SnS-1 and R-SnS-3 materials are that it is a better electrical conductor, and most importantly, thin films can be readily fabricated for device applications by simply warming the sample to its liquid crystalline state. Thin films of the material are expected to provide more sensitive and faster response to small and large molecule analytes.

4 3D Tin sulfide frameworks

In contrast to the 2D tin sulfide-based structures, 3D tin(IV) thiostannates are relatively rare, so far only two structure types have been reported. A summary of their structural characteristics is given in Table 4. $K_2Sn_2S_5$ was prepared by heating a mixture of Sn, K_2S, and S in an evacuated, sealed Pyrex tube at 320 °C.[33] The 3D framework of $(Sn_2S_5)^{2-}$ is presented in Fig. 11. It is built entirely from trigonal-bipyramidal SnS_5. The SnS_5 building units form through edge-sharing, zig-zag chains running along the *a* axis as highlighted in Fig. 11. They are bridged by sulfide ligands to yield 12-membered channels running down the *b* axis, with charge-compensating K^+ cations snugly fitting inside. As shown in Fig. 12, the structure of $Na_4Sn_3S_8$ [34] is closely related to that of $K_2Sn_2S_5$. The only difference is that in $Na_4Sn_3S_8$, the zig-zag chains are linked together by tetrahedral SnS_4 spacer units, leaving two terminal sulfurs located in the channels (Fig. 12). The charge-balancing Na^+ cations reside inside the channels. Although both materials appear to have an open channel structure, the charge-balancing cations fit tightly inside the channels, and they are thus actually quite dense. $Tl_2Sn_2S_5$, isostructural with $K_2Sn_2S_5$, has been crystallized by heating a stoichiometric mixture of Tl, Sn and S powders at 350 °C.[35] In view of the similar diameters of K^+ (1.52 Å) and Tl^+ (1.54 Å), but the smaller size of Na^+ (1.16 Å),[36] the formation of the $Na_4Sn_3S_8$ structure, with two large terminal sulfurs located inside of the channel, suggests that the tin sulfide-based all-inorganic frameworks favors a dense-packed, rather than an open structure.

Table 4 A summary of 3D tin(IV) thiostannates

chemical formula	coordination number		synthetic character of structure	technique
	Sn	S		
$K_2Sn_2S_5$	5	2	12-membered channel	solid state
$Na_4Sn_3S_8$	4, 5	1, 2	14-membered channel	solid state

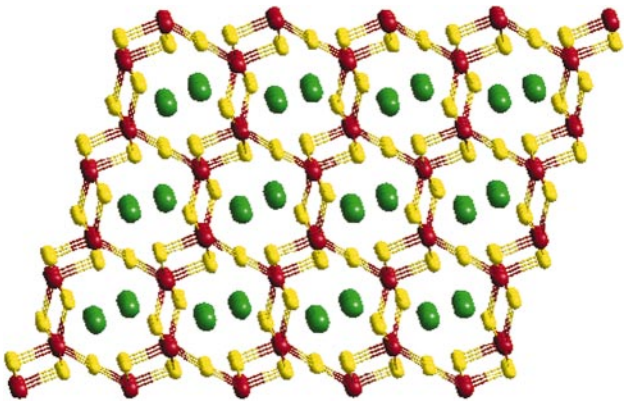

Fig. 11 An illustration of the channel structure of $K_2Sn_2S_5$, viewed down the *b* axis[33]

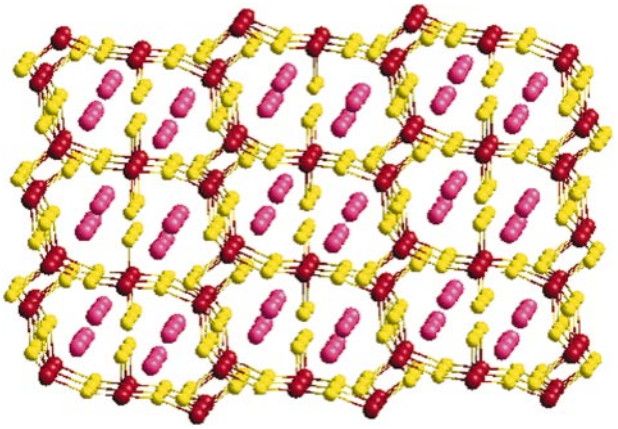

Fig. 12 An illustration of the channel structure of $Na_4Sn_3S_8$, viewed down the *b* axis[34]

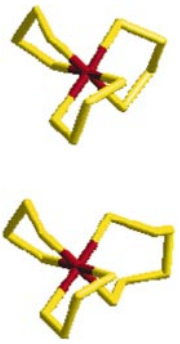

Fig. 13 Structures of $[Sn(S_4)_3]^{2-}$ and $[Sn(S_4)_2S_6]^{2-}$ [38]

5 Tin(IV) polythiostannates

Discrete and polymeric tin(IV) polythiostannates have been characterized with varied polysulfide ligand chain lengths and geometric tin sites, see Table 5. The best known discrete tin(IV) polythiostannate anions are $[Sn(S_4)_3]^{2-}$ and $[Sn(S_4)_2S_6]^{2-}$, both having an octahedral tin(IV) site. The former contains three bidentate tetrasulfide ligands, while the latter has two bidentate tetrasulfide and one bidentate hexasulfide ligand, Fig. 13. Interestingly, these two anions often co-crystallize in a single unit cell to form a disordered structure. For example, in $(Et_4N)_2[Sn(S_4)_3]_{0.4}[Sn(S_4)_2S_6]_{0.6}$, the $[Sn(S_4)_3]^{2-}$ and $[Sn(S_4)_2S_6]^{2-}$ moieties are found to be located at the same crystallographic site with a partial occupancy of 0.4 and 0.6, respectively;[37] while in $[DABCOH]_2[Sn(S_4)_3]_{0.5}[Sn(S_4)_2S_6]_{0.5}$, they each have a partial occupancy of 0.5.[27,38],

In contrast to the discrete $[Sn(S_4)_3]^{2-}$ and $[Sn(S_4)_2S_6]^{2-}$ anions, β-$Rb_2Sn_2S_8$ features an extended 2D framework as displayed in Fig. 14.[33] It contains octahedral and tetrahedral tin(IV) sites. The basic building units can be viewed as face-sharing double semi-broken cubes that are linked *via.* double bridge $Sn(\mu\text{-}S)_2Sn$ sulfur bonds to create parallel chains along the *a* axis direction. These chains are cross-linked by tetrasulfide S_4 ligands to yield the elaborate 2D structure of β-$K_2Sn_2S_8$. The charge-compensating cation, Rb^+ resides between the tin(IV) polysulfide sheets. The linkage between the

Table 5 A summary of representative tin(IV) polysulfide structures

chemical formula	structure dimensionality	tin sulfide polyhedra	polysulfide ligands
$[Sn(S_4)_3]^{2-}$	monomer	SnS_6	S_4
$[Sn(S_4)_2S_6]^{2-}$	monomer	SnS_6	S_6
$Rb_2Sn_2S_8$	2D framework	SnS_6, SnS_4	S_4
$Cs_2Sn_2S_6$	2D framework	SnS_5	S_2

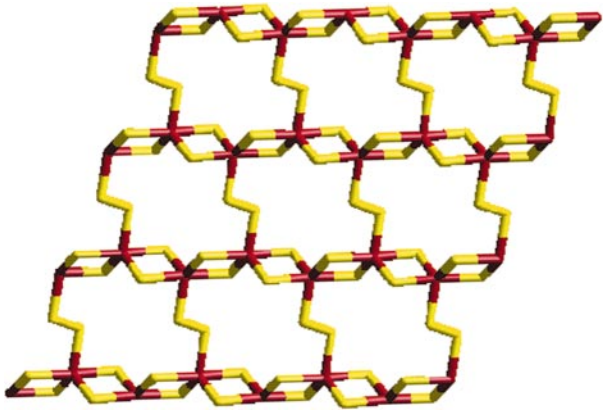

Fig. 14 A representation of the 2D open structure of $K_2Sn_2S_8$, the K^+ cations are omitted for clarity (note the tetrapolysulfide ligand)[33]

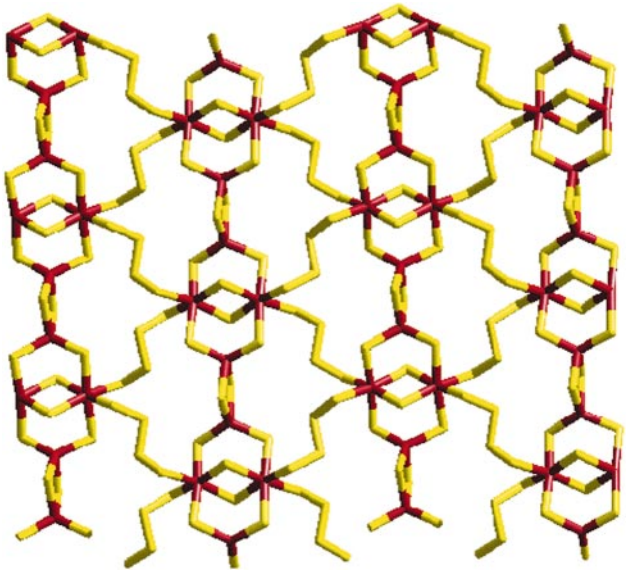

Fig. 15 A representation of the 2D open structure of $Cs_2Sn_2S_6$, the Cs^+ cations are omitted for clarity (note the disulfide ligand)[33]

chains through the S_4 ligands is rather flexible. In this context, it has been found that a polytype of β-$Rb_2Sn_2S_8$, namely α-$Rb_2Sn_2S_8$, can be crystallized from an identical reaction mixture to that used to prepare β-$Rb_2Sn_2S_8$ but at a slightly lower temperature.[33] In comparison with monoclinic α-$Rb_2Sn_2S_8$, the high-temperature product has its layers slightly shifted along the [1 0 2] crystallographic axis to form a more symmetric, *i.e.* orthorhombic, lattice.

$Cs_2Sn_2S_6$ also features a 2D framework as shown in Fig. 15.[33] However, in this case, it contains one unique trigonal bipyramidal tin(IV) site which shares two common edges to form polymeric chains along the *c* axis. These chains are cross-linked by disulfide S_2 ligands to form arrays of 14-membered distorted rectangular pores parallel to the [1 0 0] plane. It is clear that tin polysulfides have a diverse bonding character and many more new structures are expected to emerge with different polysulfide ligands and coordination geometries around the tin centers.

6 Ternary tin sulfides

All the aforementioned structures contain only tin–sulfide covalent bonds, and the metal and organic cations in the structure are ionically bonded to the tin(IV) thio- and polythiostannate anions to compensate the charge. However, a large number of ternary tin sulfide $Sn_xS_yA_z$ systems (A represents any elements other than tin or sulfur) have been studied in

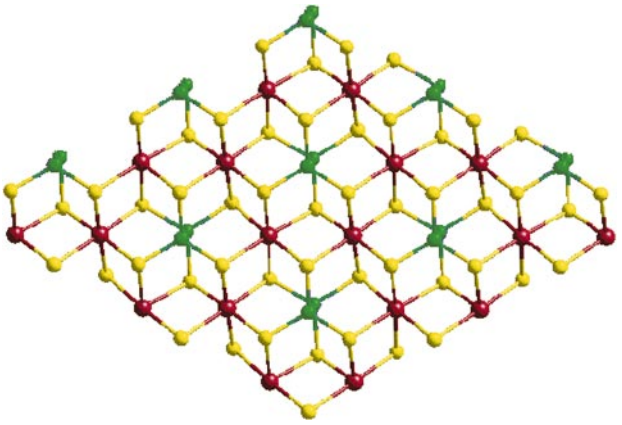

Fig. 16 An illustration of the layered structure of the rhombohedral $Sn_2P_2S_6$. Note that it is similar to the berndtite SnS_2 structure shown in Fig. 5, but with one half of the octahedral tin sites replaced by P_2.[42]

which the element A is covalently bonded to Sn and/or S. Most ternary tin sulfides are metal tin sulfides, and were prepared through a conventional direct reaction of stoichiometric SnS_x ($x = 1, 2$) with M_ySz, or elements Sn, M, and S in an evacuated ampoule at elevated temperatures. A large collection of metals has been studied, including Na, K, Ba, In, Tl, Ge, Pb, Sb, Mn, Cu, and Eu.[39] As the applied reaction temperature is normally high, up to 1000 °C, most of the produced materials feature a dense packed 2- or 3D structure. For example, $CuSn_{3.75}S_8$ has been synthesized by reacting elements Cu, Sn, and S at 1100 °C. It has a defect spinel structure, with Sn^{IV} occupying 15/16 of the octahedral and Cu^{I} residing in 1/2 of the tetrahedral sites.[40] Na_2SnS_3 was prepared by melting a stoichiometric mixture of SnS_2 and Na_2S at 750 °C, followed by slow cooling to room temperature at 16 °C h^{-1}.[41] It has a NaCl type structure with tin and sodium distributed over the cation positions.

Recently, non-metal elements have also been sucessfully introduced into tin sulfide-based frameworks. For example, crystals of $Sn_2P_2S_6$ have been prepared from stoichiometric Sn, P, and S elements sealed in a quartz tube and heated at high temperatures.[42] Three polymorphic $Sn_2P_2S_6$ phases have been reported, two of which, monoclinic(I) and rhombohedral, display a 2D structure similar to bulk berndtite SnS_2, where 50% of the octahedral metal sites are, however, replaced by P_2 (Fig. 16). By contrast, the monoclinic(II) phase consists of discrete $P_2S_6^{4-}$ anions that are linked together *via* weak S—Sn interactions.[43] In all of these phases, the oxidation state of tin atoms is tin(II). Recently, SnP_2S_6 was synthesized under similar reaction condition as $Sn_2P_2S_6$, but with a reduced tin content of Sn : P : S of 1 : 2 : 6 in the reaction mixture.[44] SnP_2S_6 has an ordered defect structure of the $Fe_2P_2S_6$ structure type. The tin centers are in the +4 oxidation state, half of the metal sites are thus vacant and this results in a 2D open structure (Fig. 17). Both SnP_2S_6 and $Sn_2P_2S_6$ are found to display interesting non-linear optical properties.[45]

Solid solutions of $SnS_{2-x}Se_x$ ($0 \leqslant x \leqslant 2$) and $(Me_4N)_2Sn_3S_{7-x}Se_x$ ($0 \leqslant x \leqslant 7$) families have been synthesized.[16,46,47] All members of the $SnS_{2-x}Se_x$ series crystallize in the $Cd(OH)_2$ type structure, as shown in Fig. 5, to yield an isostructural family of solid solutions, *i.e.* sulfur and selenium are randomly distributed over the chalcogenide sites in the lattice.[16,46] The intercalation chemistry of the $SnS_{2-x}Se_x$ series has been investigated by O'Hare and co-workers. They have successfully included cobaltocene [$Co(\eta$-$Cp)_2$] into the van der Waals' gaps between the tin chalcogenide layers, to form a series of $SnS_{2-x}Se_x\{Co(\eta\text{-}Cp)_2\}_{0.33\pm0.02}$ materials. Through X-ray and neutron diffraction and ^2H solid state NMR studies, it was found that the cobaltocene is ordered in the tin chalcogenide gap, with the C_5 axis of the η-Cp ring parallel to

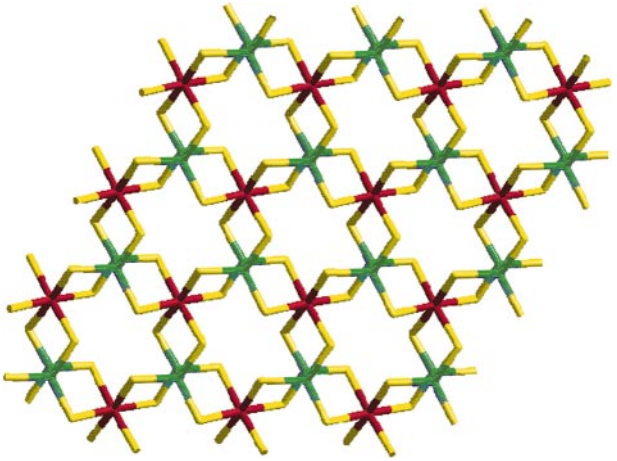

Fig. 17 An illustration of the 2D open structure of SnP_2S_6. Note that this structure is related to the $Sn_2P_2S_6$ structure shown in Fig. 15, but half of the octahedral tin sites are vacant.[44]

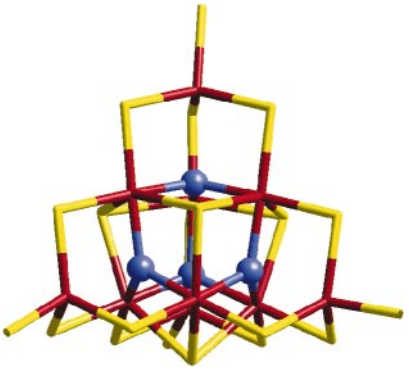

Fig. 18 Structure of the supercluster $(Sn_{10}O_4S_{20})^{8-}$ [48]

the layers. In the intercalated materials, Sn^{IV} in the host layers is partially reduced to Sn^{II} as seen by Mössbauer spectroscopy. The conductivities of both the host and the host–guest intercalated series were studied through variable temperature single crystal measurements. The intercalated materials display reduced resistivity in comparison with the hosts. Remarkably, the high selenium content members, *i.e.* $SnS_{2-x}Se_x\{Co(\eta\text{-}Cp)_2\}_{0.33\pm0.02}$ ($1.85 \leqslant x \leqslant 2$), exhibit superconductivity at temperatures below 6 K. In comparison, the $(Me_4N)_2Sn_3S_{7-x}Se_x$ ($0 \leqslant x \leqslant 7$) family has a 2D open structure.[47a] It displays a similar framework architecture to that of the SnS-1 material displayed in Fig. 8. The $(Me_4N)_2Sn_3S_{7-x}Se_x$ series is found to crystallize in an orthorhombic space group, $P2_12_12_1$. The optical absorption edge of the $(Me_4N)_2Sn_3S_{7-x}Se_x$ series is found to display a monotonic red shift with increasing Se content as found in the isostructural $SnS_{2-x}Se_x$ family. The results of a detailed recent study[47b] show that the distribution of the chalcogenides in $(Me_4N)_2Sn_3S_{7-x}Se_x$ is random (solid-solution, Vegard law) at the length scale of the unit cell but site-selective at the level of the trigonal bipyrimidal building-blocks.

In addition to the mixed sulfur–selenium based materials, tin oxy-sulfides have also been reported. For example, the 'supertetrahedron' $(Sn_{10}O_4S_{20})^{8-}$ has been crystallized as a discrete anion in $Na_8Sn_{10}O_4S_{20}\cdot 32H_2O$ and $Cs_8Sn_{10}O_4S_{20}\cdot 13H_2O$ compounds.[48] The $(Sn_{10}O_4S_{20})^{8-}$ cluster is built of ten corner-sharing SnS_4 tetrahedrons, Fig. 18. Four oxygen atoms are located in the supertetrahedral voids and are coordinated to six of the ten tin atoms to form SnS_4O_2 distorted octahedra. Recently, these supertetrahedral clusters have been linked together through sulfur bridging bonds to give rise to 2D and 3D open-framework structures. In

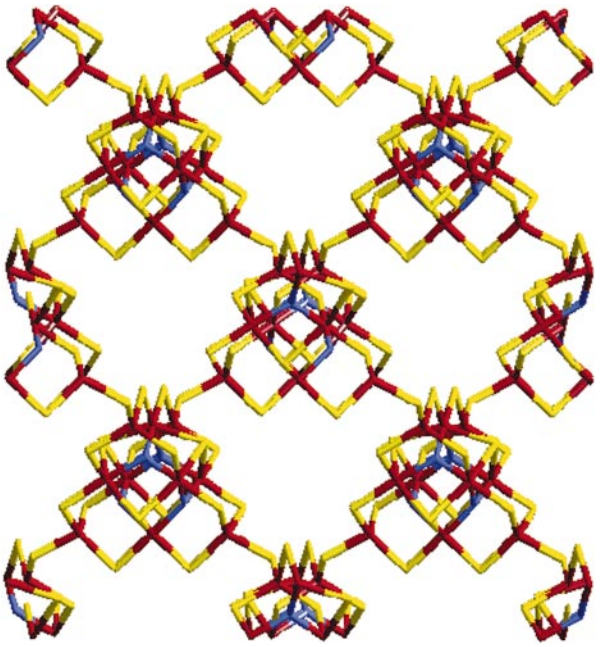

Fig. 19 A representation of the open-framework structure of $[Sn_5S_9O_2][HN(CH_3)_3]_2$, for clarity showing only one of the interpenetrated diamond-type tin sulfide networks[50]

$[Sn_{20}S_{37}O_8]^{10-}$, each $(Sn_{10}O_4S_{20})^{8-}$ is connected to three neighboring $(Sn_{10}O_4S_{20})^{8-}$ clusters through corner-sharing of the sulfur apex to form a 2D open-framework structure,[49] while in $[Sn_5O_2S_9][HN(CH_3)_3]_2$, each $(Sn_{10}O_4S_{20})^{8-}$ being linked to four neighboring $(Sn_{10}O_4S_{20})^{8-}$ clusters to form two interwoven diamond-type structures Fig. 19.[50] It is interesting to mention that the $(Sn_4Se_{10}O)^{6-}$ tetrameric-unit has recently been synthesized in this laboratory, a reduced size version of the supertetrahedral $(Sn_{10}O_4S_{20})^{8-}$ cluster.[51] In $(Sn_4Se_{10}O)^{6-}$, the tin selenide cluster has an adamantane structure and the oxygen is located in the central tetrahedral void and coordinated to the four tin apexes to make them five-coordinated. The $(Sn_4Se_{10}O)^{6-}$ clusters are linked together through the four terminal seleniums to distorted tetrahedral Sn^{IV} centres to form $(Sn_5Se_{10}O)^{2-}$, a 3D open-framework diamond-type structure where the charge balance is maintained by two $(CH_3)_4N^+$ cations occupying the void spaces (Fig. 20).

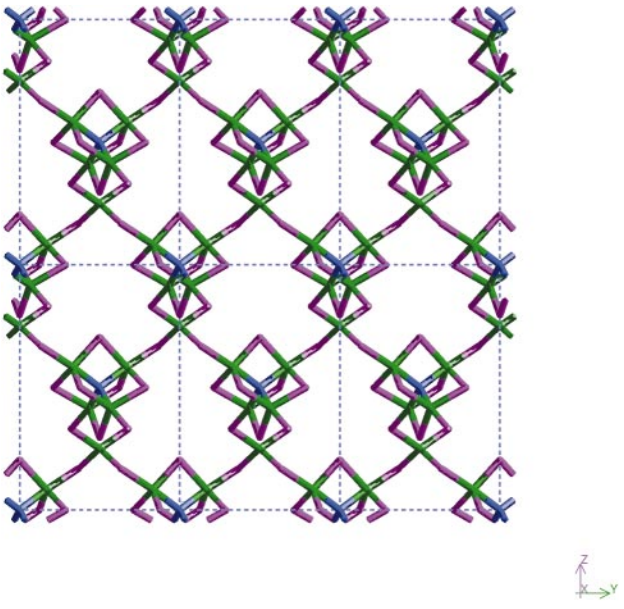

Fig. 20 An illustration of the 3D open framework structure of $(Me_4N)_2(Sn_5Se_{10}O)$. The Me_4N^+ cations are omitted for clarity.[51]

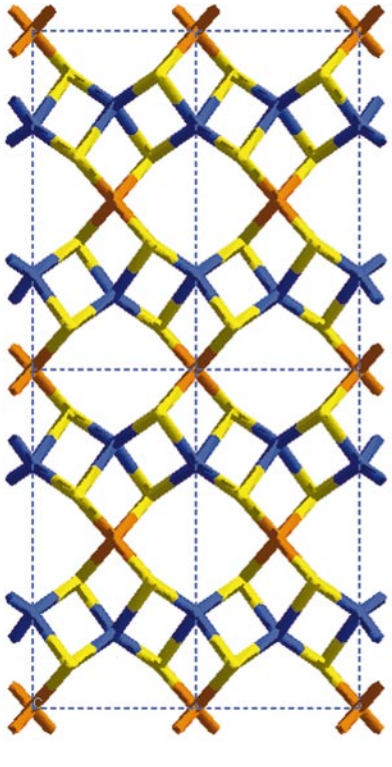

Fig. 21 A representaion of the 2D open structure of $Rb_2Cu_2SnS_4$. Rb^+ cations residing between the $(Cu_2SnS_4)^{2-}$ sheets are omitted.[52]

7 Quatenary tin sulfides

Quaternary $Rb_2Cu_2SnS_4$ and $Rb_2Cu_2Sn_2S_6$ have been synthesized by heating Sn and Cu powder in a Rb_2S_5 flux at 400 °C.[52] In both materials, tetrahedral SnS_4 and CuS_4 units are the basic building blocks. The edge sharing of SnS_4 and CuS_4 creates a 2D open structure of $Rb_2Cu_2SnS_4$ with 8-atom rings (Fig. 21). The rubidium cations are located between the anionic layers of $[Cu_2SnS_4]^{2-}$ to balance the charge. The corner sharing of SnS_4 and CuS_4 results in the 2D open struuture of $A_2Cu_2Sn_2S_6$ (Fig. 22). It can be viewed as a derivative of a 3D zinc blende adamantane-type structure material of formula Cu_2SnS_3. However, the replacement of half of the Cu atoms in Cu_2SnS_3 by alkali-metal atoms reduces the dimensionality of the framework structure from three to two due to the interruption of covalent bonding through the structure. Each $[Cu_2Sn_2S_6]^{2-}$ slab contains three metal layers, *i.e.* a Cu layer sandwiched by two Sn metal layers in which one-half of the Sn sites are missing to form parallel grooves. The Rb^+ cations are located inside the grooves. $K_2Au_2SnS_4$ and $K_2Au_2Sn_2S_6$ were obtained by heating Sn and Au powder at 350 °C in a K_2S_5 and K_2S_9 flux, respectively.[52] As shown in Fig. 23(A), the 1D structure of the former is constituted by tetrahedral SnS_4 and linear AuS_2 building blocks in a ratio of 1:2. The paralell zig-zag $[Au_2SnS_4]^{2-}$ chains are separated by K^+ cations. $K_2Au_2Sn_2S_6$ is constructed from dimeric Sn_2S_6 units that are linked together by linear Au atoms to form fully extended infinite chains, Fig. 23(B). Note that although these two materials have similar chemical formulae to those of the Cu analogs discussed above, they present completely different structures due to the different preferred coordination geometries of Cu^I and Au^I. The former favors a tetrahedral coordination environment while the latter favours a linear geometry.

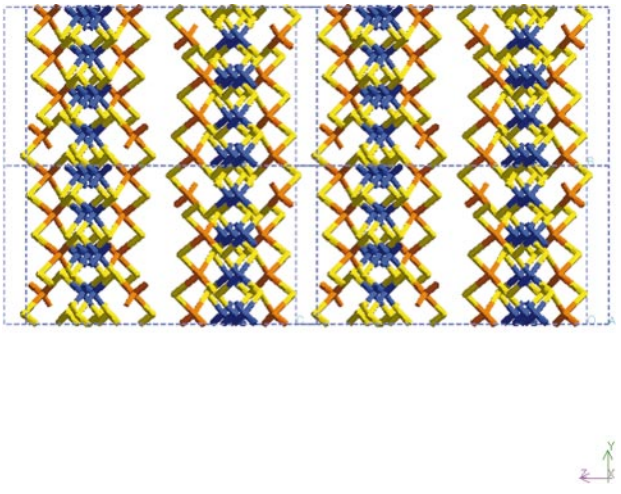

Fig. 22 A representaion of the 2D open structure of $Rb_2Cu_2Sn_2S_6$ viewed parallel to the layers[52]

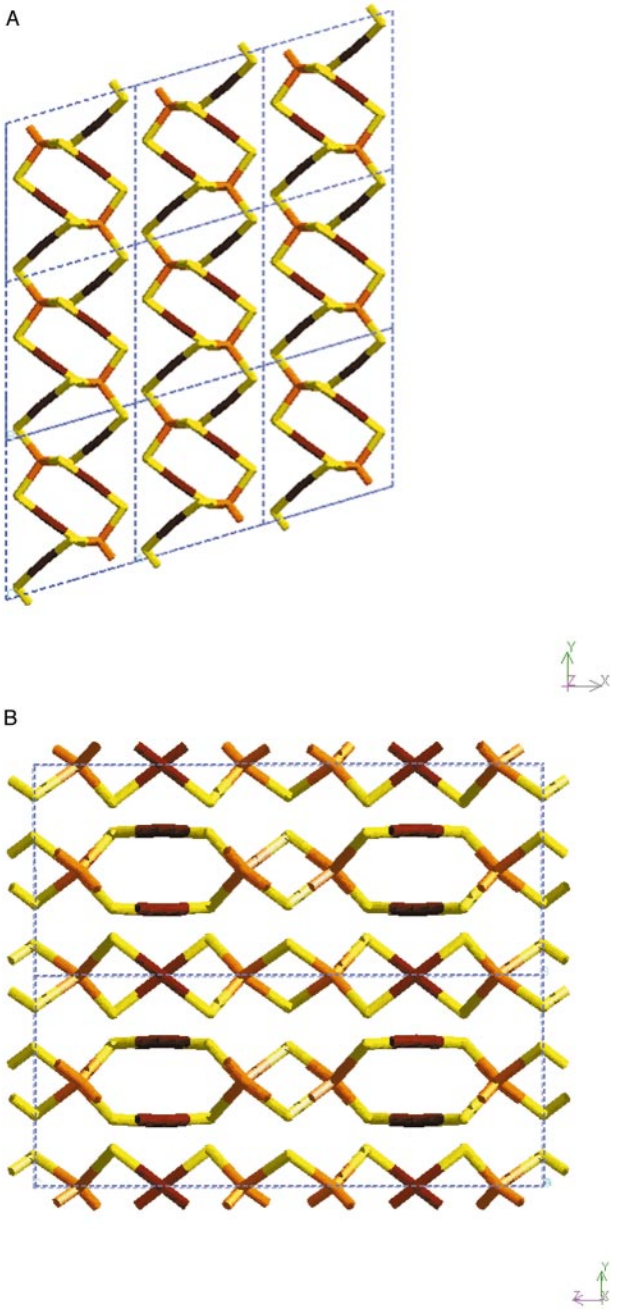

Fig. 23 An illustration of the chain structures of (A) $K_2Au_2SnS_4$ and (B) $K_2Au_2Sn_2S_6$. The K^+ cations residing between the chains are omitted for clarity.[52]

8 Conclusion

Representative tin sulfide-based materials that have appeared in the recent materials chemistry literature, ranging from molecular species to 1D chain, 2D dense and porous sheets and 3D open frameworks, have been reviewed. In particular, 'soft chemistry approaches' such as hydro- and solvothermal synthesis, and the molten-salt flux technique, have generated a large collection of novel microporous tin (poly)sulfide materials and the first example of a mesoporous tin sulfide, which present interesting optical, electrical, adsorption and liquid crystal properties. In the 1D, 2D and 3D extended tin (poly)sulfides, molecular tin sulfide species, $[SnS_4]^{4-}$, $[Sn_2S_6]^{4-}$ and $[Sn_4S_{10}]^{4-}$ are found to serve as structure building blocks. This suggests that by employing modular-assembly synthetic approaches, in combination with templating agents, many more novel binary, ternary, quaternary tin sulfide structures are expected to emerge with desired properties and functions, for the development of a range of new sensing, separation and catalysis applications.

The financial assistance of the Natural Sciences and Engineering Research Council of Canada (NSERC) is deeply appreciated. T.J. expresses her gratitude to University of Toronto for an Open Fellowship held through the course of her PhD study.

References

1 (*a*) N. N. Greenwood and A. Earnshaw, *The Chemistry of the Elements*, Pergamon Press, New York, 1984, ch. 10 and 15; (*b*) B. Krebs, *Z. Anorg. Allg. Chem.*, 1983, **22**, 113; (*c*) D. J. Vaughan and J. R. Craig, *Mineral Chemistry of Metal Sulfides*, Cambridge University Press, Cambridge, 1978.
2 P. G. Harrison, *Chemistry of Tin*, Blackie, Glasgow, 1989.
3 N. N. Greenwood and A. Earnshaw, A. *The Chemistry of the Elements*, Pergamon Press, New York, 1984, p. 780.
4 B. Krebs and W. Schiwy, *Z. Anorg. Allg. Chem.* 1973, **398**, 63.
5 (*a*) R. L. Bedard, L. D. Vail, S. T. Wilson and E. M. Flanigen, *US Patent*, 4 880 761, 1989; R. L. Bedard, L. D. Vail, S. T. Wilson and E. M. Flanigen, *US Patent*, 4 933 068, 1990; R. L. Bedard, S. T. Wilson, L. D. Vail, J. M. Bennett and E. M. Flanigen, in *Zeolites: Facts, Figures, Future*, ed. P. A. Jacobs and R. A. van Santen, *Stud. Surf. Sci. Catal.*, Elsevier Science Publishers B. V., Amsterdam, 1989, vol. 49, part A, p. 375; (*b*) W. S. Sheldrick and B. Schaaf, *Z. Naturforsch. Teil B*, 1994, **49**, 655; (*c*) W. S. Sheldrick and M. Wachhold, *Angew. Chem., Int. Ed. Engl.*, 1997, **36**, 206.
6 (*a*) M. G. Kanatzidis, *Chem. Mater.*, 1990, **2**, 353; (*b*) S. Dhingra and M. G. Kanatzidis, *Science*, 1992, **258**, 1769; (*c*) M. G. Kanatzidis and C. Sutorik, *Prog. Inorg. Chem.*, 1995, **43**, 151.
7 R. L. Bedard, G. A. Ozin, H. Ahari, C. L. Bowes, T. Jiang and D. Young, *US Patent*, 5 594 263, 1997.
8 W. Z. Schiwy, S. Pohl and B. Krebs, *Z. Anorg. Allg. Chem.*, 1973, **402**, 77.
9 (*a*) B. Krebs, S. Pohl and W. Schiwy, *Z. Anorg. Allg. Chem.* 1972, **393**, 241; (*b*) B. Krebs, S. Pohl, S. and W. Schiwy, *Angew. Chem., Int. Ed. Engl.*, 1970, **9**, 897.
10 B. Krebs and W. Schiwy, *Z. Anorg. Allg. Chem.*, 1973, **63**, 398.
11 W. Z. Schiwy, C. Blutau, D. Gäthje and B. Krebs, *Z. Anorg. Allg. Chem.*, 1975, **412**, 1.
12 G. H. Moh, *Neus Jahrb. Mineral. Abh.*, 1969, **111**, 227.
13 R. Kniep, D. Mootz, U. Severin and H. Wunderlich, *Acta Crystallogr., Sect. B*, 1982, **38**, 2022; D. Mootz and H. Puhl, *Acta Crystallogr., Sect. B*, 1967, **23**, 471.
14 R. Herzenberg, *Rev. Mineral.*, 1932, **4**, 33.
15 (*a*) H. Wiedemeier and F. J. Csillag, *Z. Kristallogr.*, 1979, **149**, 17; (*b*) H. G. von Schnering and H. Wiedemeier, *Z. Kristallogr.*, 1981, **156**, 143.
15 P. Woulfe, *Philos. Trans. R. Soc. London*, 1771, **61**, 114.
16 H. P. B. Rimmington and A. A. Balchin, *J. Cryst. Growth.*, 1972, **15**, 51.
17 B. Palosz, W. Steurer and H. Schulz, *Acta Crystallogr., Sect. B*, 1990, **46**, 449.
18 B. Palosz, W. Palosz and S. Gierlotka, *Acta Crystallogr., Sect. B*, 1986, **42**, 653.
19 A. R. Verma and P. Krishna, *Polymorphism and Polytypism in Crystals*, John Wiley & Sons, New York, 1969.
20 H. Jagodzinski, *Neues Jahrb. Mineral. Abh.*, 1954, **3**, 49.
21 B. Palosz, W. Steurer and H. Schulz, *Acta Crystallogr., Sect. B.*, 1990, **46**, 449.
22 W. S. Sheldrick and B. Schaaf, *Z. Anorg. Allg. Chem.*, 1994, **620**, 1041.
23 W. S. Sheldrick, *Z. Anorg. Allg. Chem.*, 1988, **562**, 23.
24 C. Bowes, PhD Thesis University of Toronto, 1996.
25 T. Tan, Y. Ko and J. B. Parise, *Acta Crystallogr., Sect. C*, 1995, **51**, 398.
26 J. B. Parise, Y. Ko, J. Rijssenbeek, D. M. Nellis K. Tan and S. Koch, *J. Chem. Soc., Chem. Commun.*, 1994, 527.
27 (*a*) T. Jiang, PhD Thesis University of Toronto, 1997; (*b*) T. Jiang, A. J. Lough, G. A. Ozin, R. L. Bedard and R. W. Broach, *J. Mater. Chem.*, 1998, **8**, 721; T. Jiang, A. Lough and G. A. Ozin, *Adv. Mater.*, 1998, **10**, 42.
28 (*a*) T. Jiang, A. J. Lough, G. A. Ozin, D. Young and R. L. Bedard, *Chem. Mater.*, 1995, **7**, 245; (*b*) Y. Ko, K. Tan, D. M. Nellis, S. Koch and J. B. Parise, *J. Solid State Chem.*, 1995, **114**, 506.
29 G. A. Marking and M. G. Kanatzidis, *Chem. Mater.* 1995, **7**, 1915.
30 (*a*) D. R. Corbin, L. Abrams, G. A. Johns, M. M. Eddy, W. T. A. Harrison, G. D. Stucky and D. E. Cox, *J. Am. Chem. Soc.*, 1990, **112**, 4821; (*b*) C. A. Fyfe, H. Strobl, G. Kokotailo, G. J. Kennedy and G. E. Barlow, *J. Am. Chem. Soc.*, 1988, **110**, 3373.
31 (*a*) H. Ahari, C. L. Bowes, T. Jiang, A. Lough, G. A. Ozin, R. L. Bedard, S. Petrov and D. Young, *Adv. Mater.*, 1995, **7**, 375; (*b*) G. A. Ozin, *Supramol. Chem.*, 1995, **6**, 125.
32 T. Jiang and G. A. Ozin, *J. Mater. Chem.*, 1997, **7**, 2213.
33 J. Liao, C. Varotsis and M. G. Kanatzidis, *Inorg. Chem.*, 1993, **32**, 2453.
34 J.-C. Jumas, E. Philippot and M. Maurd, *J. Solid State Chem.*, 1975, **14**, 152.
35 G. Eulenberger, *Z. Naturforsch., Terl B*, 1981, **36**, 687.
36 (*a*) F. A. Cotton, G. Wilkinson and P. L. Gaus, *Basic Inorganic Chemistry*, John Wiley & Sons, New York, 1987; (*b*) J. E. Huheey, *Inorganic Chemistry: Principles of Structure and Reactivity*, Harper & Row, New York, 1983, p. 258.
37 A. Müller, J. Schimanski, M. Römer, H. Bögge, W. Baumann, W. Eltzner, E. Krickemeyer and U. Billerbeck, *Chimia*, 1985, **39**, 25.
38 T. Jiang, G. A. Ozin and R. L. Bedard, *Adv. Mater.*, 1994, **6**, 860; T. Jiang, G. A. Ozin, A. Lough and R. L. Bedard, *J. Mater. Chem.*, in press.
39 J. Olivier-Fourcade, J. C. Jumas, M. Ribes, E. Philippot and M. Maurin, *J. Solid State Chem.*, 1978, **23**, 155.
40 S. Jaulmes, M. Julien-Pouzol, J. Rivet, J. C. Jumas and M. Maurin, *Acta Crystallogr., Sect. B*, 1982, **39**, 51.
41 W. Mark, O. Lindqvist, J. C. Jumas and E. Philippot, *Acta Crystallogr., Sect. B*, 1974, **30**, 2620.
42 V. W. Klingen, R. Ott and H. Hahn, *Z. Anorg. Allg. Chem.*, 1973, **396**, 271.
43 V. W. Klingen, G. Eulenberger and H. Hahn, *Z. Anorg. Allg. Chem.*, 1973, **401**, 97; H. P. B. Rimmington and A. A. Balchin, *Phys. Status Solidi,* 1971, **7**, K47.
44 Z. Wang, R. D. Willett, R. A. Laitinen and D. A. Cleary, *Chem. Mater.*, 1995, **7**, 856.
45 D. A. Cleary, R. D. Willett, F. Ghebremichael and M. Kuzyk, *Solid State Commun.*, 1993, **88**, 39.
46 D. O'Hare, *Chem. Rev.*, 1992, 121 and references therein.
47 (*a*) H. Ahari, G. A. Ozin, R. L. Bedard, S. Petrov and D. Young, *Adv. Chem.*, 1995, **7**, 370; (*b*) H. Ahari, Ö. Dag, A. G. Ozin, S. Petrov and R. L. Bedard, *J. Phys. Chem.*, in press.
48 W. Schiwy and B. Krebs, *Z. Angew. Chem.*, 1975, **87**, 451.
49 J. B. Parise, Y. Ko, K. Tan, D. M. Nellis and S. Koch, *J. Solid State Chem.*, 1995, **117**, 219.
50 J. B. Parise and Y. Ko, *Chem. Mater.*, 1994, **6**, 718.
51 H. Ahari, A. Lough and G. Ozin, unpublished work.
52 J. H. Liao and M. G. Kanatzidis, *Chem. Mater.*, 1993, **5**, 1561.

Paper 7/09054D; *Received* 17*th December*, 1997